ENVIRONMENTAL RESEARCH LETTERS

LETTER • OPEN ACCESS

Improving analogues-based detection & attribution approaches for hurricanes

To cite this article: Stella Bourdin *et al* 2025 *Environ. Res. Lett.* **20** 024042

ENVIRONMENTAL RESEARCH
LETTERS

CrossMark

OPEN ACCESS

RECEIVED
12 November 2024

REVISED
9 January 2025

ACCEPTED FOR PUBLICATION
15 January 2025

PUBLISHED
30 January 2025

LETTER

Improving analogues-based detection & attribution approaches for hurricanes

Stella Bourdin[1,*], Suzana J Camargo[3], Chia-Ying Lee[3], Jonathan Lin[4], Mathieu Vrac[2], Pradeebane Vaittinada Ayar[2] and Davide Faranda[2,5,6]

[1] Atmospheric, Oceanic and Planetary Physics, Department of Physics, University of Oxford, Oxford, United Kingdom
[2] Laboratoire des Sciences du Climat et de l'Environnement, Université Paris-Saclay & IPSL, UMR 8212 CEA-CNRS-UVSQ, Gif-sur-Yvette, France
[3] Lamont-Doherty Earth Observatory, Columbia University, Palisades, NY, United States of America
[4] Department of Earth and Atmospheric Sciences, Cornell University, Ithaca, NY, United States of America
[5] London Mathematical Laboratory, 8 Margravine Gardens, London W6 8RH, United Kingdom
[6] Laboratoire de Météorologie Dynamique/IPSL, École Normale Supérieure, PSL Research University, Sorbonne Université, École Polytechnique, IP Paris, CNRS, Paris, France
[*] Author to whom any correspondence should be addressed.

E-mail: stella.bourdin@physics.ox.ac.uk

Keywords: hurricane, attribution, extreme events, tropical cyclone, synthetic tracks

Supplementary material for this article is available online

Abstract

This paper presents a proof of concept for a new analogue-based framework for the detection and attribution of hurricane-related hazards. This framework addresses two important limitations of existing analogue-based methodologies: the lack of observed similar events, and the unsuitability of the distance metrics for hurricanes. To do so, we use a track-based metric, and we make use of synthetic tracks catalogues. We show that our method allows for selecting a sufficient number of suitable analogues, and we apply it to nine hurricane cases. Our analysis does not reveal any robust changes in wind hazards, translation speed, seasonality, or frequency over recent decades, consistent with current literature. This framework provides a reliable alternative to traditional analogue-based methods in the case of hurricanes, complementing and potentially enhancing efforts in addressing extreme weather event attribution.

1. Introduction

Extreme weather events' increasing frequency and/or intensity are among the most visible and impactful effects of climate change [1, 2]. In this context, extreme event attribution aims to assess the influence of human-induced climate change against natural variability in the occurrence and intensity of specific extreme events [3].

Hurricanes (tropical cyclones in the North Atlantic Ocean) are the most devastating extreme weather events, with the potential to cause significant social and economic impacts [4]. In the context of climate change, we know that the proportion of major hurricanes is likely to increase [1], but we do not know how the frequency of these events will change [5, 6].

To this date, it remains difficult to detect and attribute changes in hurricane climatology [7]. In the Atlantic, a statistically significant trend is found in the percentage of Category 4–5, but not in the mean intensity of hurricanes [8, 9]. While a slowing trend in hurricanes translation speed over the North American coast has been noticed [10], multiple studies mentioned that this trend could be due to related changes in satellite data and hurricane detection techniques [11–14]. Regarding seasonality, an expansion of the Atlantic hurricane season has been found in observations, in particular with more early-season hurricanes [15, 16].

There are only few studies attempting to attribute individual hurricanes, using probabilistic attribution [17, 18], and storyline-based methods [19–23]. They all but one [19] focused on precipitation. In most

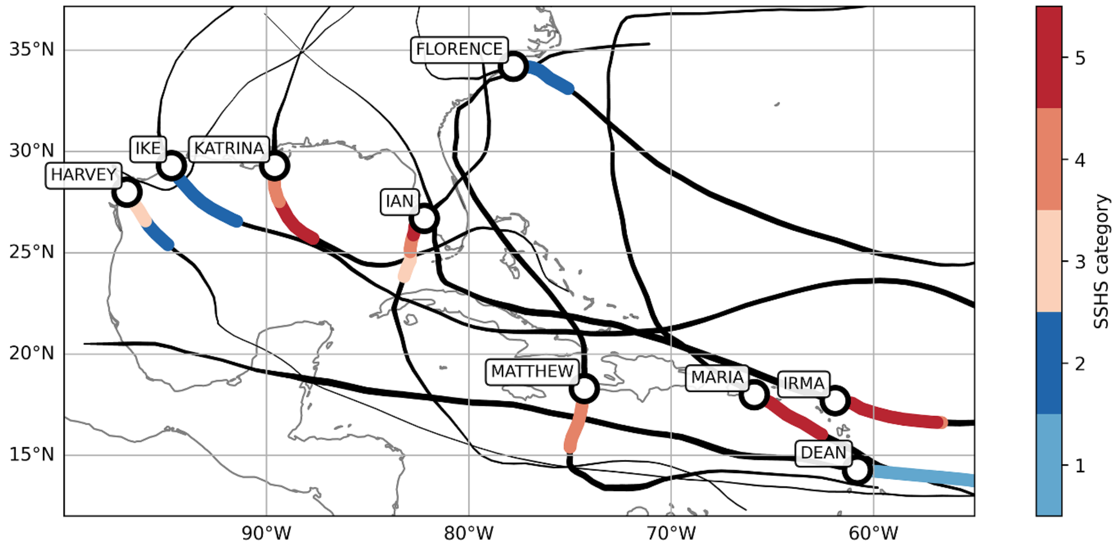

Figure 1. Hurricane cases in this study. Full tracks are shown in black with width proportional to intensity. Tracks 24 h before landfall are colored by Saffir–Simpson Hurricane Scale (SSHS) category. Dark circles show the landfall points considered in this study.

cases, they found that climate change was responsible for making precipitation more extreme. While this is in line with the understanding of the thermodynamics of climate change, several studies find increases that are beyond the sole Clausius–Clapeyron effect [17, 18, 21, 24]. No robust change was found for other characteristics than precipitation and storm surge.

Analogue-based attribution is a type of storyline attribution which has been used extensively for the attribution of extreme events such as heat waves to anthropogenic climate change [25, 26], but never to hurricanes. In analogues-based attribution, we compare the hazards and impacts of events resulting from similar atmospheric conditions. In most cases, such events are found in historical records, and a 'factual' period corresponding to the present climate with anthropogenic climate change is compared to a 'counterfactual' period corresponding to a past climate with less anthropogenic climate change. A strength of this approach is that it uses existing data rather than running event-specific simulations. This allows analogue-based methods to be used in rapid attribution, which is currently done by the 'ClimaMeter' consortium for publishing routine press releases on impact extreme events through www.climameter.org (see section 2.1, [27]). However, while analogues have been extensively used in the mid-latitude by conditioning on the synoptic-scale flow as defined by sea-level pressure (SLP) or mid-tropospheric geopotential, whether they work in the tropics remains to be assessed.

In this paper, we assess the suitability of the analogues methodology for hurricane hazard attribution, showing that with the current ClimaMeter framework, there is a systematic lack of confidence in the detected changes because of the lack of analogues (section 2). We then propose an alternative analogue-based framework that uses synthetic track catalogues and a track-based distance metric (section 3). We apply this framework to detect changes in hazards related to recent Atlantic hurricanes, focusing on changes in the wind speed of hurricanes, as well as their probability of occurrence, translation speed and seasonality (section 4).

For conciseness, our discussion mostly consists of the case of Hurricane Irma, focusing on its first landfall on Barbuda on 6 September, 2017. However, nine cases were analyzed, shown in figure 1, and figures for all cases analyzed can be found in the supplementary material. Landfall coordinates and characteristics for all cases, as well as the rationale for choice, are described in table A1.

2. ClimaMeter

2.1. Description

ClimaMeter offers a dynamic approach to perform a detection attribution analysis of weather extremes within a climate context [27]. Here, we analyse how tropical cyclones have changed in the 'factual' recent period (1987–2023) compared the 'counter-factual' previous past decades (1950–1986). To do so, we selected the 35 best analogues of MSLP anomalies between August to November associated with the target cases in the ERA5 reanalysis [28]. The anomalies are computed against the 1950–2023 climatology over a $10 \times 10^{\circ}$ box centered on the location of the storm's minimum pressure. Then, we search for significant differences between present and past analogues in terms of pressure and wind speed (wspd).

Following [26], we define analogue quality Q as the average Euclidean distance of a given event from

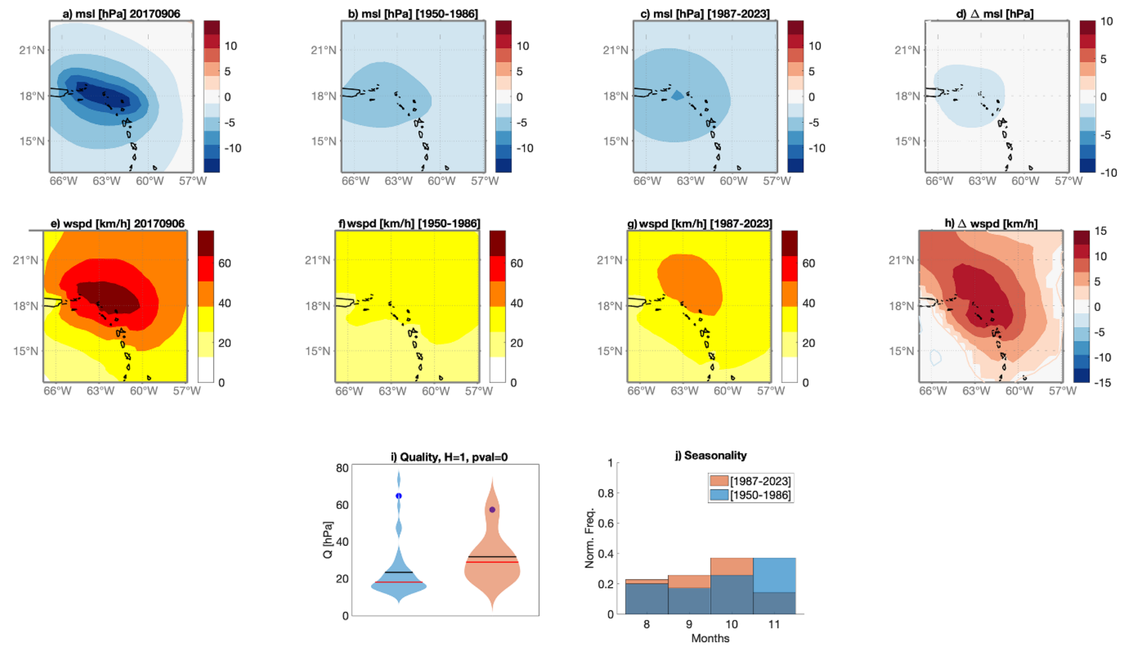

Figure 2. ERA5 Analogues Analysis for 6 September 2017 and the region defined by [66.9W 56.9W 12.7E 22.7E] and the hurricane season ASON. a–d: sea-level pressure (msl) anomaly during the event (a), averaged over the counter-factual (b) and factual (c) analogues, and changes between factual and counter-factual analogues (Δmsl) (d). In (d) colour-filled areas indicate significant anomalies with respect to the bootstrap procedure. e–h: Same as a–d but for wind speed (wspd). i: Distribution of counterfactual (blue) and factual (orange) analogue quality Q. A blue dot marks values for the peak day of the extreme event. Horizontal bars correspond to the mean (black) and median (red) of the distributions. j: Distribution of analogues in each month.

its closest 35 analogues. If the target event's Q belongs to the distribution of its analogues', then that event is not considered unprecedented, and attribution can be performed. If not, the event is considered unprecedented and, therefore, not attributable.

For more technical details regarding the methodology, please see [27]. Note that the ClimaMeter framework provides more indicators than what is presented, but we focus on pressure and wind speed because these are the outputs available for other models used in this paper

ClimaMeter is the baseline for our study. We assess its suitability for hurricane-related wind hazard attribution in the next subsection.

2.2. Analysis for Irma

In figure 2 we show the results of this analysis for Hurricane Irma while it is over the Caribbean on 6 September, 2017.

Panels (d) and (h) show that Irma's analogues have deeper ($\approx$2 hPa) pressure minima and are associated with more intense winds ($\approx$10 km h^{-1}) in the factual period, compared with the counter-factual period.

Panel (i) shows that the Irma's Q value is well above the distribution of its analogues'. This is true for both period, although less so in the factual period.

We also find that events similar to Irma have become less frequent in November, while they previously mainly occurred in September and October (figure 2(j)).

2.3. Limitations of the current ClimaMeter approach

The main shortcoming of the above analysis is the low quality of the analogues, yielding low confidence in the outcome of ClimaMeter. This is true for the nine studied hurricanes cases here (see supplementary material), and this is a systematic outcome for hurricane cases in the reports published in the ClimaMeter websiste.

Low quality means the selected analogues do not resemble the actual event. In fact, about half of them do not correspond to recorded tropical cyclones. If we take Irma's analogues check whether they correspond to a tropical cyclone in IBTrACS, we find a match for 10/35 counterfactual analogues and 28/35 factual analogues.

The low quality of the analogues stems from several factors:

(i) ERA5 does not faithfully represent the structure of tropical cyclones and largely underestimates their intensity [29].
(ii) Even if most observed events can be found in ERA5 [30], hurricanes are rare events. There are only 16.0 tropical storms of which 7.7 hurricanes on average every year in the whole Atlantic basin (based on recorded storms in IBTrACS over the 1980–2021 period).
(iii) The SLP-based distance metric for cases like tropical cyclones, which can reach very low-pressure values, will necessarily yield large distance values. In the case of Irma, the pressure

anomaly is up to −15 hPa, and the detected change is of the order of 2 hPa, while the event's distance to its analogues is about 60 hPa in both periods. Moreover, this imposes collocation of events, which in our case might not be so important.

In the following, we propose a new analogue-based framework that addresses these three limitations: (i) we use observed hurricane tracks directly to overcome ERA5's limitations, (ii) we use synthetic tracks to expand the number of events, and (iii) we use a track-based distance.

3. Alternative framework

Analogues-based detection and attribution methodologies rely on the choice of a catalogue and a distance metric. Our suggestion is to use synthetic tracks as a catalogue and a track-based distance metric. The specific catalogues used below are opportunistic, and the metric is kept simple in order to provide a proof of concept.

3.1. Track catalogues

The analogues method requires the definition of a catalogue of events, which is browsed to find similar events. In our alternative framework, events are necessarily tropical cyclones, which are found in different types of track catalogues, described below.

3.1.1. Observations

Addressing limitation (i), instead of using reanalysis as a reference for real-world hurricanes, we use observed hurricane best tracks. We retrieve them from the National Hurricane Center's best-track hurricane database [HURDAT, 31] through the International Best Track Archive for Climate Stewardship [IBTrACS, 32, 33]. In the Atlantic, the record is generally considered reliable since 1950. However, there are inhomogeneities between the pre- and post-satellite eras, as we will highlight below.

3.1.2. Synthetic tracks

In any case, the number of observed hurricanes remains small (ii). Therefore, we use the synthetic track to expand the sample. Synthetic tracks are model-produced realistic tracks. Synthetic tracks were already used in the attribution of Harvey by [20], but in a probabilistic attribution framework.

Such tracks can be produced by statistical, statistical-dynamical or fully dynamical models. Here, we use tracks from three models belonging to the two latter categories.

3.1.2.1. CHAZ

The Columbia HAZard model, CHAZ, is an open-source statistical-dynamical downscaling model [34]. As such, CHAZ links physical relationships between large-scale climate drivers and TC development. The model seeds weak disturbances at a rate determined by the Tropical Cyclone Genesis Index [TCGI, 35, 36]. These disturbances are then pushed by the background steering flow, following a version of the Beta and Advection Model developed by [37]. The disturbances' intensity is modelled using an auto-regressive stochastic intensity model by [38, 39].

In this study, we use synthetic CHAZ TCs downscaled from the ERA5 reanalysis [28], similar to the dataset used by [40]. We generated 60 track ensembles for the period of 1951–2019. While each synthetic TC track has 40 intensity ensembles, here we only consider the first intensity ensemble member.

3.1.2.2. MIT open source downscaling model

We also use tracks from the MIT-Open model [41], which is an open-source derivative of the MIT (Massachusetts Institute of Technology) TC downscaling model [42]. The MIT-Open model is conceptually similar to CHAZ, but they differ in storm formation and evolution calculation. On a high level, MIT-Open randomly seeds weak proto-vortices. It then evolves these weak seeds in space and time according to the large-scale environmental flow (as represented by ERA5). Tropical cyclones move according to the beta-and-advection model [43], and intensify/decay according to the FAST intensity model [44]. For more details, the reader is referred to [41].

The MIT-Open dataset used hereafter was generated using ERA5 as input, like CHAZ.

3.1.2.3. SEAS5-20 C hindcasts

Lastly, we use unseen TC tracks from seasonal hindcasts covering the 20th century (20 C) [45]. Hindcasts are initialized forecast model runs used to verify a prediction system's performance against existing observations. For these hindcasts, the European Center for Medium-Range Forecast's fifth-generation seasonal forecast system (SEAS5) was used [46]. The SEAS5-20 C hindcasts [47] was chosen due to its length, covering the whole 20th century. The hindcasts consist of two-year forecasts with 10 ensemble members. Forecasts are initialized in May and November each year between 1901 and 2010, with initial states from CERA-20 C [Coupled European ReAnalysis of the 20th century, 48]. The atmospheric component has a resolution of 50 km (T199).

In the present work, we only consider the hurricane tracks simulated during the months of June to November in the first year of the May initialized forecasts—hence with a lead time of one month with respect to the Atlantic TC season. Not using the first month of forecast allows us to make sure that the hurricanes we study were not in the initialisation and are purely synthetic. This selection means we have 10 ensemble members per hurricane season. The TCs were detected and tracked using the TRACK algorithm [49].

3.1.3. Periods

For IBTrACS, CHAZ and MIT-Open, the years 1950–1984 are chosen for the counterfactual period, and 1985–2019 for the factual period, splitting in two the common available period. For SEAS5-20 C, we take advantage of the long span of the dataset and use 1901–1955 as counterfactual and 1956–2010 as factual. Due to different natural and forced variability over these periods, it means the same changes might not be detected in the catalogues. However, since we do not attempt any actual attribution here, we argue that using as much as the sample as possible is more important for our methodological discussion.

3.2. Track-based distance metric for analogues selection

3.2.1. Motivation

To overcome limitations in using SLP-based analogues (iii), we suggest switching to an alternative track-based distance metric for analogue selection.

ClimaMeter identifies similar days based on SLP patterns at the time of hurricane landfall. This approach seeks to match depressions with atmospheric conditions resembling those of the target hurricane. In the following, we propose to look for tropical storms with trajectories similar to those of a given hurricane, similarly what was done [50] for extra-tropical cyclones. This means that we are conditioning on the type of event (tropical storms) and their approach towards the coast. We argue that this object-oriented approach should yield greater confidence in the results. Potential changes in analogue characteristics with time are more likely to be relevant for the target event if there is a physical consistency in the type of event analogues represent. Moreover, we know that the direction of a hurricane at landfall is important for hazard patterns, as the surface wind speed has an asymmetrical footprint [51, 52].

This track-based metric also has the advantage of being usable for datasets that do not provide full physical fields but only track data—which is the case for all of the catalogues above except SEAS5-20 C. For data in the form of spatial, physical fields, it means that tropical cyclones need to be tracked beforehand.

Also, in the standard ClimaMeter method, the 35 closest analogues are selected, and the quality is checked posteriorly. Here, we reverse the paradigm: we impose a level of quality and check posteriorly that we have enough analogues. The level of quality is imposed by selecting analogues within a given distance $d_{\max}$ of the target event. Previous studies on analogue-based attribution showed that approximately 30 analogues or more per period are desirable for a robust statistical analysis [26, 27].

3.2.2. Implementation

In the following, all track data are interpolated to 1 h. We define a cyclone C as an ensemble of points in time and space: $C = (c_i)_{i\in[\![1,N_C]\!]}$, where N_C is the number of hours for which the cyclone has been recorded.

Let $H = (h_i)_{i\in[\![1,N_H]\!]}$ be the hurricane that we are targeting, with $h_l\,(l \in [\![1,N_H]\!])$ the landfall point. For each cyclone C in a track catalogue, we find c_l the closest point in space to h_l (based on the haversine distance). We then define the distance d between C and H as :

$$d(H,C) = \frac{1}{24}\sum_{k=0}^{23} ||h_{l-k}, c_{l-k}||,$$

where $||\cdot||$ is the haversine distance in space. This procedure is illustrated in figure A1.

We define the analogues of H as all cyclones C such that $0 < d(H,C) < d_{\max}$, where $d_{\max}$ is a maximum distance selected arbitrarily for each catalogue to optimize the number and quality of analogues, specified in table 1. The first inequality prevents us from including the target case in the analogues. The method is designed to select as analogues cyclones with a close landfall location and a track that has a similar approach to H. To illustrate this, figure 3 shows the selected analogues for three cases.

3.3. Validation

In this section, we demonstrate the ability of this new framework to select good-quality analogues.

The number of analogues found in each catalogue and for each period is shown in table 1. Comparing the number of analogues among the cases reflects how 'unusual' their trajectory was: hurricanes like Maria, Dean and Irma yield the highest number of analogues for all catalogues because they had very typical westward trajectories in the Caribbean. In contrast, Hurricane Matthew, which had a northward approach to Haiti, has much fewer analogues in all catalogues.

Figure 3 shows the tracks of the analogues found in each catalogue for three selected cases (figures A2 & A3 shows them for all nine cases). Irma has the most analogues across all catalogues. In figure 3, we show that in all catalogues there are analogues with westward trajectories similar to Irma's observed track, but refining $d_{\max}$ allows for tightening them around the observed track. In particular, we find analogues with landfall locations closer to Irma's observed landfall. Katrina has an intermediate number of analogues across all catalogues. In the case of IBTrACS, there are 78 analogues with tracks spread across the Gulf of Mexico; using STGs leads to a selection of analogues with tracks that are closer to that of Katrina itself, with landfall within 300 km of Katrina's landfall position.

Table 1. Number of analogues selected for each case and each catalogue. Cases are ordered by the number of analogues in IBTrACS for the factual period. Numbers below 30 are printed in italic with a star(GCD stands for Great Circle Distance).

	IBTrACS		CHAZ		MIT-Open		SEAS5-20 C	
$d_{\max}$ (°GCD)	4°		0.75°		0.75°		1°	
#TC/year	13		339		504		131	
	CF	F	CF	F	CF	F	CF	F
IRMA	21^{*}	68	87	89	249	231	162	198
DEAN	14^{*}	67	96	110	223	201	87	89
MARIA	21^{*}	64	50	50	216	168	60	57
KATRINA	19^{*}	59	66	60	138	104	19^{*}	37
IAN	17^{*}	53	27^{*}	50	109	106	18^{*}	30
FLORENCE	26^{*}	49	14^{*}	13^{*}	12^{*}	13^{*}	5^{*}	10^{*}
IKE	23^{*}	44	67	69	109	107	29^{*}	36
HARVEY	19^{*}	37	44	57	65	98	43	43
MATTHEW	4^{*}	26^{*}	6^{*}	13^{*}	15^{*}	26^{*}	4^{*}	8^{*}

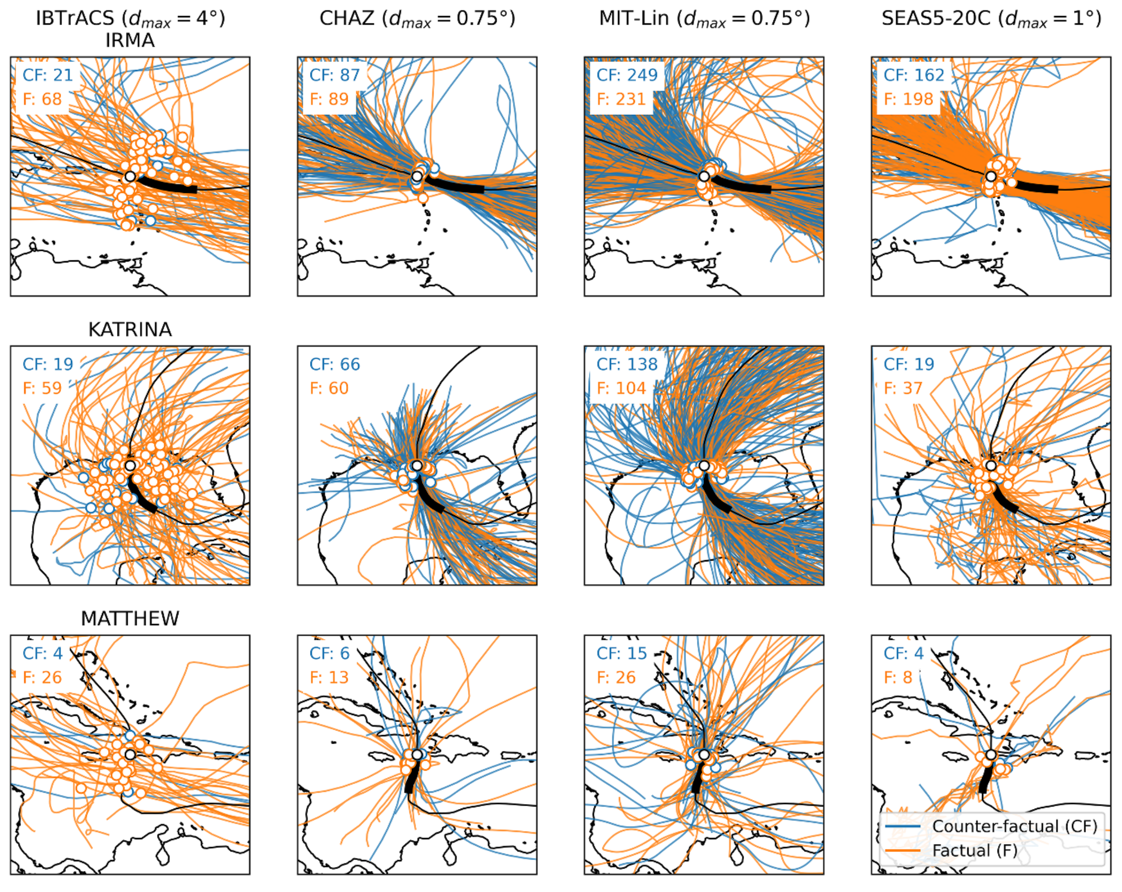

Figure 3. Analogues for hurricanes Irma (top), Katrina (middle) and Matthew (bottom), in each catalogue (columns). Counter-factual analogues are in blue and factual ones in orange. The black track is the observed hurricane track. The numbers on the top-left of each panel are the number of analogues for each period. Tracks for all analogues are shown in figures A2 & A3.

Matthew has the fewest number of analogues across all catalogues due to its unusual northward trajectory. In IBTrACS, 30 analogues were found, but the permissive $d_{\max}$ allowed for track analogues following with different direction and that do not hit Haiti. In CHAZ and SEAS5-20 C, there are fewer analogues than in other cases, but they do have similar trajectories as the observed track and do make landfall in Haiti. The very large track sample size produced by the MIT-Open model yields 41 analogues, highlighting the usefulness of a very high sample size for events with unusual tracks.

We see from this analysis that, in general, the larger the sample size in a catalogue, the smaller the value of $d_{\max}$ that can be used, which is beneficial for analogue quality.

Here the 30 analogues threshold is attained for several cases, including Irma, so we can move forward with our analysis of hazard changes.

4. Changes in hurricane characteristics

Having demonstrated the suitability of our framework, we apply it to the detection of potential changes in the characteristics of the tracks of Irma's and eight other hurricane analogues.

In figure 4, we compare the characteristics of the analogues in the factual and counter-factual periods for Irma, which has the most analogues across catalogues. The number of Irma's analogues in all catalogues but IBTrACS is well above 30. For IBTrACS, the counter-factual only has 21 analogues, but we show it here nonetheless for completeness because it is an observational reference, because it gives the opportunity for a discussion on the homogeneity of the dataset, and because it illustrates well the advantage of using synthetic tracks. Similar figures for all cases can be found in the supplementary material and we provide a conclusion over all cases for each studied characteristic below.

4.1. Number of analogues per period

First we analyze whether there is a significant change in the number of analogues between the two periods, a statistically significant increase in the number of analogues would indicate an increase in the likelihood of similar events—and vice-versa. In the case of Irma, there is no statistically significant change in the number of analogues, except in the case of IBTrACS (figure 4, top row). It should be noted that a significant increase in the number of IBTrACS analogues in the factual period is found for all cases analyzed. This is more likely due to instrumentation-related inhomogeneities in the best-track dataset [53] than an actual change in the likelihood of those events between the two periods.

Two other statistically significant increases in the number of analogues are found (table A2): Hurricane Ian's analogues in CHAZ and Hurricane Harvey's analogues in MIT-Open, and Hurricane Katrina's analogues in SEAS5-20 C. Note that the p-values remain above 1%, and these changes are not robust across multiple catalogues, so we conclude that they are more likely to be spurious.

4.2. Intensity

Next, we examine whether the intensity of the events has changed across the two periods. Intensity, as measured by the analogue's maximum wind speed, Irma's analogues do not have a statistically significant change in wind speed in any of the catalogues (figure 4, second row). A statistically significant decrease in wind speeds associated with Ike's analogues is found in IBTrACS but is likely spurious owing to the low number of analogues and the well-known technological changes present in best-track datasets [53] (table A3).

Intensity, as measured by minimum SLP, is available only for IBTrACS and SEAS-20 C. A statistically significant decrease is found in Katrina's analogues' minimum SLP in SEAS5-20 C (table A4). It means that Katrina's analogues are more intense in the factual period (first half of the 20th century for SEAS5-20 C) compared to the counterfactual (second half of the 20th century).

4.3. Translation speed

Translation speed is a crucial characteristic of hurricane tracks, as stalling hurricanes are more likely to cause large accumulated precipitation values at a given location, such as in the case of Hurricane Harvey.

In our analysis, no statistically significant change is found in translation speed for Irma's analogues in any catalogue (figure 4, third row). Changes in translation speed are detected for Ian's analogues in IBTrACS and Florence's analogues in SEAS5-20 C (table A5).

This is particularly interesting as there is a controversy regarding changes in TC translation speed. Kossin [10] found a detectable change in observed translation speed globally. Still, this result could be dependent on the period used in the analysis [11, 12] and is not present in some model simulations in the historical period [13]. Hassanzadeh *et al* [14] shows that the climate change impact on TC translation speed may be regionally dependent. In the present analysis, we find a statistically significant reduction in the translation speed of Ian's analogues in observations, which is not found using other catalogues nor for other cases. This is interesting in the context where the case of Ian is reminiscent of Debby this year (2024), which stalled, bringing important rainfall to Florida.

4.4. Seasonality

Changes in seasonality are investigated, as hurricane characteristics and potential impacts depend on when they occur.

A significant change in seasonality is found for Irma's analogues in CHAZ only (figure 4, fourth row) and Florence's analogues in IBTrACS only (table A6). For Irma, factual analogues in CHAZ are generally found earlier in the season, with a maximum in August, compared to the counterfactual when most analogues are found in September. For Florence, factual analogues are found in IBTrACS slightly earlier in the factual compared to the counterfactual, but in both cases, the maximum is in September.

Regarding all of the above statistically significant changes highlighted, we stress that because they are not found across catalogues, we do not think this statistical significance reflects an actual robust trend. We

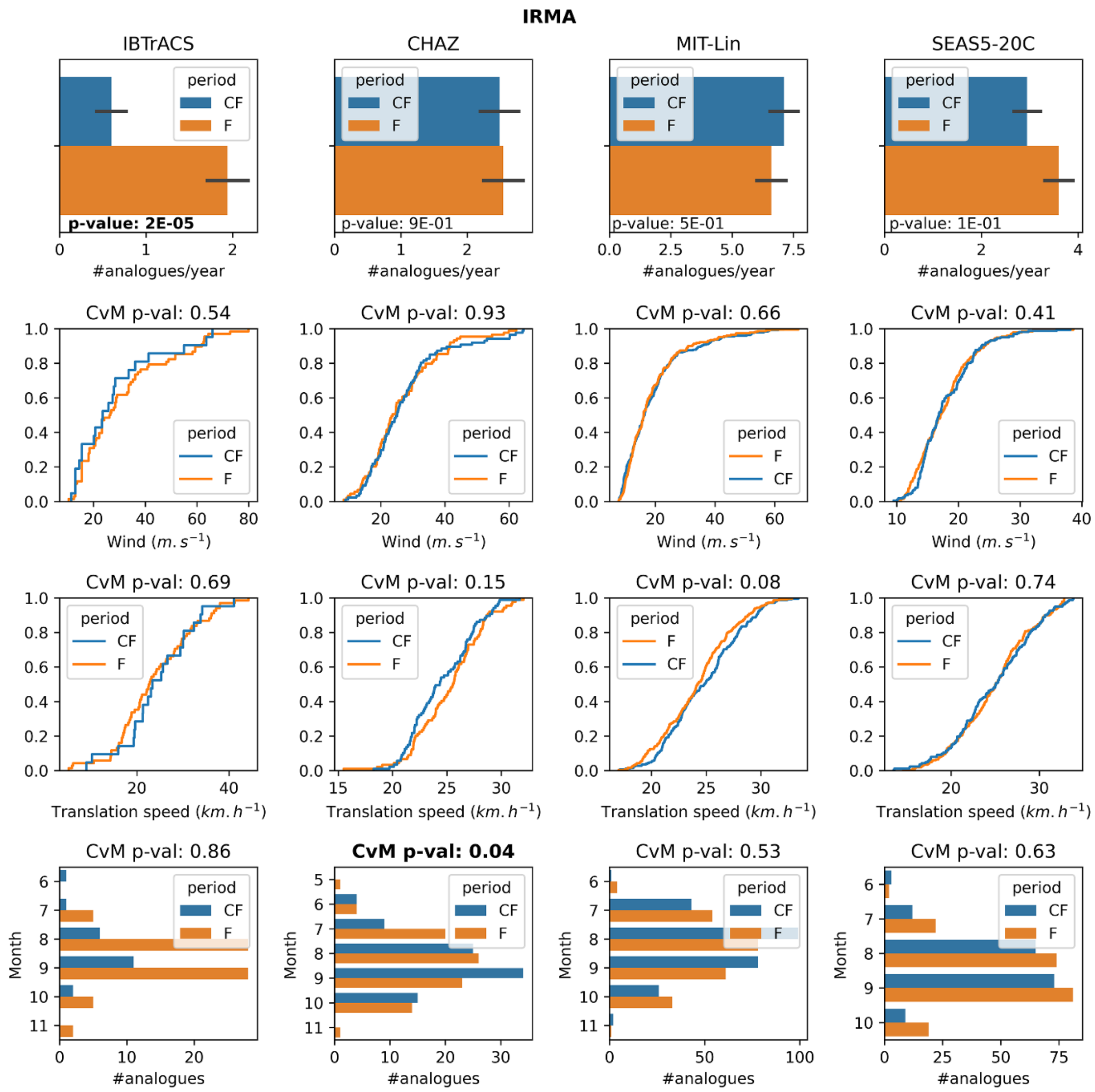

Figure 4. Characteristics of Irma's analogues in each catalogue (columns). The first line shows the number of analogues per year for each period, with the error bar showing the standard error. The p-value is shown for a T-test for the mean, in bold when statistically significant at the 5% level. The second line shows the empirical cumulative distribution functions of maximum wind speed at the surface (for SEAS5-20 C at 850 hPa). The third line shows the empirical cumulative distribution functions of the translation speed during the 24 h before landfall. The fourth line shows the month of the formation of the analogues in both periods. For lines 2–4, the results of a Cramer von Mises test are shown, which determines whether the samples in each period are drawn from different distributions, in bold when the p-value is $<$5%. In the fourth line, the test was performed for the day-of-year.

also performed sensitivity tests to the values of $d_{\max}$ that show small but existent sensitivity of the results. For that reason, we do not make any statement about a detected change in hurricane-related hazard in this study.

5. Conclusion

In this study, we propose a new analogue-based framework that can be used as a foundation for the detection and attribution of hurricane-related hazard changes. This new framework identifies analogues as tropical cyclones with similar tracks. It makes use of available synthetic track catalogues. Sampling among many more events allows us to make statements with more confidence than in the current ClimaMeter framework when dealing with tropical cyclones, as the quality of the analogues has improved. It is also very quick to run for new cases. As such, it has the potential to be used even in a rapid attribution context. Although our analysis does not include as many indicators as ClimaMeter does, most importantly precipitation and variability, these could certainly be added in the future.

A specific novelty of this work is also treating seasonal hindcasts as synthetic track generators and comparing them to statistical-dynamical STGs. While statistical-dynamical generators are fast to run, they rely on simplified assumptions, especially regarding genesis, and only include a few TC-related hazards. Seasonal prediction systems as dynamical STGs provide an alternative physically consistent framework including both wind speed, SLP and rainfall. These models are very costly to run, but such simulations can be used for many purposes.

Relying on synthetic tracks can potentially introduce biases associated with the models. However, the potential impacts of these biases are minimized by comparing tracks from a single model. Provided the biases are consistent across periods, they should not impact the differences. In some cases, however, the models' deficiencies might prevent the attribution, e.g. in the case that not enough analogues can be found for a given model.

Applying this methodology to nine hurricane cases, we do not identify any robust change in the wind hazards, probability of occurrence, translation speed or seasonality. This aligns with the existing literature, where the only signal that is robustly identified as having emerged regards precipitation [1, 7].

This work paves the way for further research in improving the detection and attribution of tropical cyclones. This constitutes a proof of concept, and there is room for improvement. For example, we deliberately chose a simple distance metric, but if one is interested in using this method for attributing downstream impacts, conditioning on intensity could be relevant, as was done in [54]. Importantly, including precipitation in our analysis would be informative, as this is the most impactful hazard, and it is expected to increase. Moreover, this method could easily be extended to future projections after carefully considering their reliability.

Data availability statement

The data that support the findings of this study will be openly available following an embargo at the following URL/DOI: 10.5281/zenodo.14102094.

Acknowledgments

This work was made possible by Institut Pascal at Université Paris-Saclay with the support of the Program TROPICANA, 'Investissements d'avenir' ANR-11-IDEX-0003-01. Additionally, all authors acknowledge useful discussions within the MedCyclones COST Action (CA19109) and the FutureMed COST Action (CA22162) communities.

SB received financial support from the NERC-NSF research Grant N° NE/W009587/1 (NERC) & AGS-2244917 (NSF) HUrricane Risk Amplification and Changing North Atlantic Natural disasters (Huracan), and from the EUR IPSL-Climate Graduate School through the ICOCYCLONES2 project, managed by the ANR under the 'Investissements d'avenir' programme with the Reference 37 ANR-11-IDEX-0004 - 17-EURE-0006. SJC and CYL acknowledge support of the National Science Foundation Grants (AGS 20-43142, 22-17618, 22-44918). DF received support from the European Union's Horizon 2020 research and innovation programme under Grant Agreement No. 101003469 (XAIDA) and from the European Union's Horizon 2020 Marie Sklodowska-Curie Grant Agreement No. 956396 (EDIPI) and the LEFE-MANU-INSU-CNRS grant 'CROIRE'. MV benefited from state aid managed by the National Research Agency under France 2030 bearing the References ANR-22-EXTR-0005 (TRACCS-PC4-EXTENDING project), and acknowledges support from the 'COESION' project funded by the French National program LEFE (Les Enveloppes Fluides et l' Environnement).

We would like to thank the editor and three anonymous reviewers for their help in making the manuscript better.

Appendix. Supplementary figures and tables

Table A1. Landfall coordinates and characteristics of the nine hurricanes studied in this article. These cases have been chosen to represent a diversity of landfall locations, as well as hurricane trajectories. We have been careful to include a few non-major hurricanes (cat. 1 or 2) (Florence and Dean) to determine if that would improve the quality of the analogues.

Name	Year	Landfall date	Long.	Lat.	SLP (hPa)	Wind (knots)	SSHS cat.
KATRINA	2005	2005-08-29 11:00:00	−89.6	29.3	919.8	110.5	4
MATTHEW	2016	2016-10-04 11:00:00	−74.3	18.3	935.0	130.0	5
IRMA	2017	2017-09-06 06:00:00	−61.9	17.7	914.0	155.0	5
MARIA	2017	2017-09-20 10:00:00	−65.9	18.0	919.4	135.2	5
IAN	2022	2022-09-28 19:00:00	−82.2	26.7	940.8	130.4	5
FLORENCE	2018	2018-09-14 11:00:00	−77.8	34.2	955.8	80.2	2
HARVEY	2017	2017-08-26 03:00:00	−96.9	28.0	937.0	115.0	4
IKE	2008	2008-09-13 07:00:00	−94.7	29.3	950.0	95.0	3
DEAN	2007	2007-08-17 09:00:00	−60.8	14.3	971.0	85.0	2

Table A2. p-values of the t-test for difference in means of sample number per period. Values below 5% are bolded with a star.

	IBTrACS	CHAZ	MIT	SEAS5
KATRINA	$\mathbf{6.8\times10^{-5}}$*	6.2×10^{-1}	1.0×10^{-1}	$\mathbf{2.6\times10^{-2}}$*
MATTHEW	$\mathbf{1.2\times10^{-4}}$*	1.9×10^{-1}	2.3×10^{-1}	2.7×10^{-1}
IRMA	$\mathbf{1.7\times10^{-5}}$*	8.9×10^{-1}	5.4×10^{-1}	1.0×10^{-1}
MARIA	$\mathbf{1.3\times10^{-5}}$*	1.0×10^{0}	5.2×10^{-2}	7.7×10^{-1}
IAN	$\mathbf{1.4\times10^{-4}}$*	$\mathbf{2.3\times10^{-2}}$*	8.8×10^{-1}	6.8×10^{-2}
FLORENCE	$\mathbf{4.4\times10^{-3}}$*	8.6×10^{-1}	8.6×10^{-1}	2.0×10^{-1}
HARVEY	$\mathbf{3.6\times10^{-2}}$*	2.9×10^{-1}	$\mathbf{4.8\times10^{-2}}$*	1.0×10^{0}
IKE	$\mathbf{3.7\times10^{-2}}$*	8.8×10^{-1}	9.1×10^{-1}	3.7×10^{-1}
DEAN	$\mathbf{8.7\times10^{-7}}$*	3.7×10^{-1}	4.7×10^{-1}	8.9×10^{-1}

Table A3. p-values of the Cramer-von-Mises for difference in distribution of wind in each period. Values below 5% are bolded with a star.

	IBTrACS	CHAZ	MIT	SEAS5
KATRINA	5.7×10^{-1}	6.8×10^{-1}	8.4×10^{-2}	3.7×10^{-1}
MATTHEW	6.8×10^{-1}	3.8×10^{-1}	5.0×10^{-1}	8.9×10^{-2}
IRMA	5.4×10^{-1}	9.3×10^{-1}	6.6×10^{-1}	4.1×10^{-1}
MARIA	3.4×10^{-1}	3.4×10^{-1}	9.4×10^{-1}	NaN
IAN	7.9×10^{-1}	1.9×10^{-1}	5.9×10^{-1}	4.6×10^{-1}
FLORENCE	2.9×10^{-1}	6.2×10^{-2}	5.9×10^{-1}	7.0×10^{-1}
HARVEY	8.8×10^{-2}	5.3×10^{-1}	3.7×10^{-1}	8.1×10^{-1}
IKE	$\mathbf{4.2\times10^{-2}}$*	8.1×10^{-1}	2.2×10^{-1}	1.8×10^{-1}
DEAN	4.4×10^{-1}	1.1×10^{-1}	5.3×10^{-1}	1.1×10^{-1}

Table A4. p-values of the Cramer-von-Mises for difference in distribution of minimum SLP in each period. Values below 5% are bolded with a star.

	IBTrACS	SEAS5
KATRINA	7.0×10^{-1}	$\mathbf{1.0\times10^{-2}}$*
MATTHEW	4.2×10^{-1}	5.5×10^{-1}
IRMA	6.6×10^{-1}	4.2×10^{-1}
MARIA	2.6×10^{-1}	5.2×10^{-1}
IAN	9.6×10^{-1}	3.5×10^{-1}
FLORENCE	4.7×10^{-1}	5.2×10^{-1}
HARVEY	2.2×10^{-1}	9.4×10^{-1}
IKE	2.2×10^{-1}	8.0×10^{-2}
DEAN	6.7×10^{-1}	7.0×10^{-1}

Table A5. p-values of the Cramer-von-Mises for difference in distribution of translation speed in each period. Values below 5% are bolded with a star.

	IBTrACS	CHAZ	MIT	SEAS5
KATRINA	4.3×10^{-1}	2.9×10^{-1}	7.5×10^{-1}	1.1×10^{-1}
MATTHEW	8.2×10^{-1}	2.2×10^{-1}	9.6×10^{-1}	3.5×10^{-1}
IRMA	6.9×10^{-1}	1.5×10^{-1}	7.5×10^{-2}	7.4×10^{-1}
MARIA	6.8×10^{-1}	7.1×10^{-1}	6.6×10^{-2}	2.9×10^{-1}
IAN	$\mathbf{6.5\times10^{-3}}*$	2.1×10^{-1}	4.7×10^{-1}	6.7×10^{-1}
FLORENCE	6.7×10^{-1}	9.8×10^{-1}	3.8×10^{-1}	7.7×10^{-2}
HARVEY	1.6×10^{-1}	8.3×10^{-2}	8.9×10^{-1}	2.0×10^{-1}
IKE	9.2×10^{-2}	5.5×10^{-1}	6.2×10^{-1}	3.6×10^{-1}
DEAN	8.0×10^{-1}	9.8×10^{-1}	2.7×10^{-1}	6.8×10^{-1}

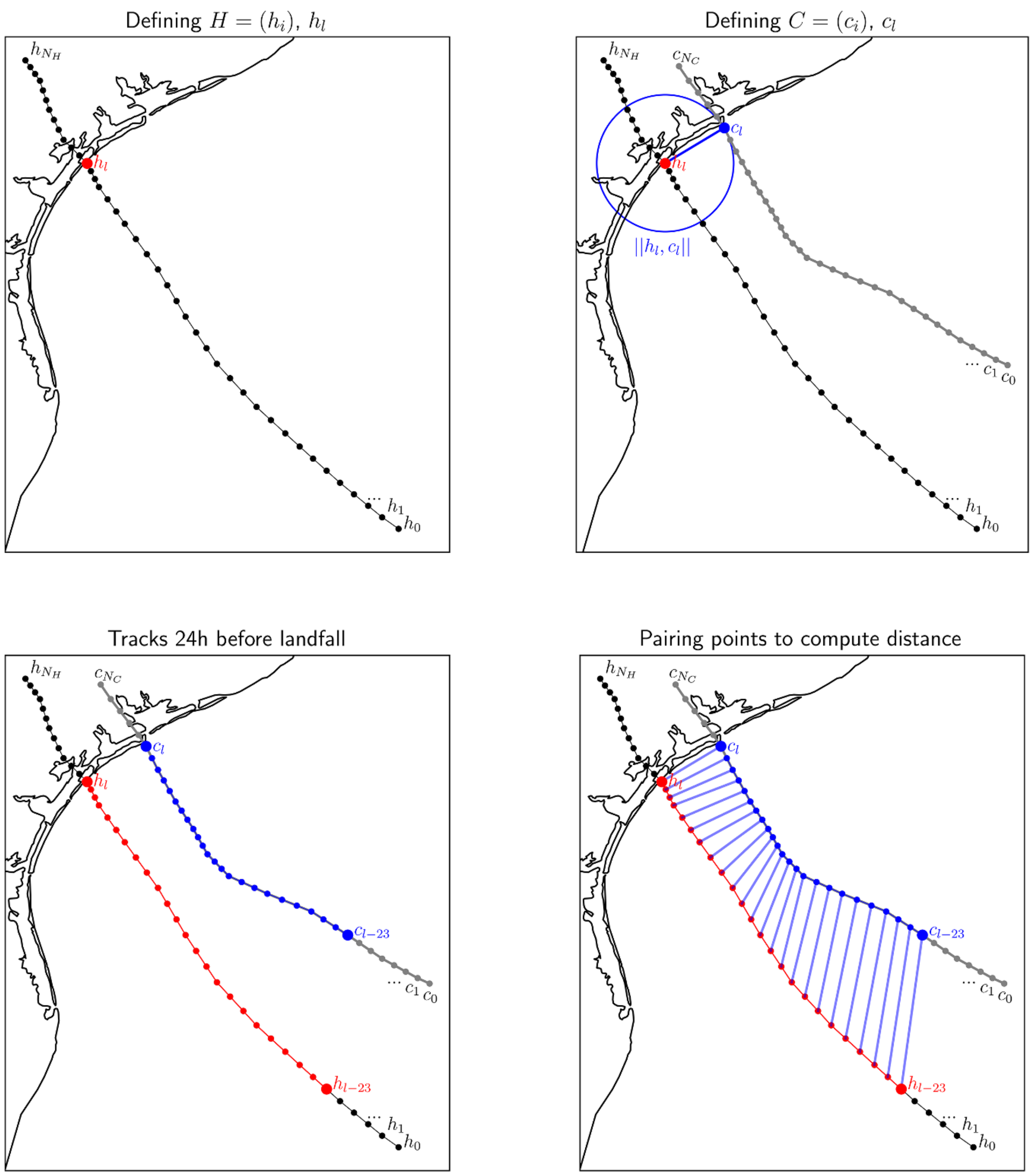

Figure A1. Illustration of the distance computation described in section 3.2.2.

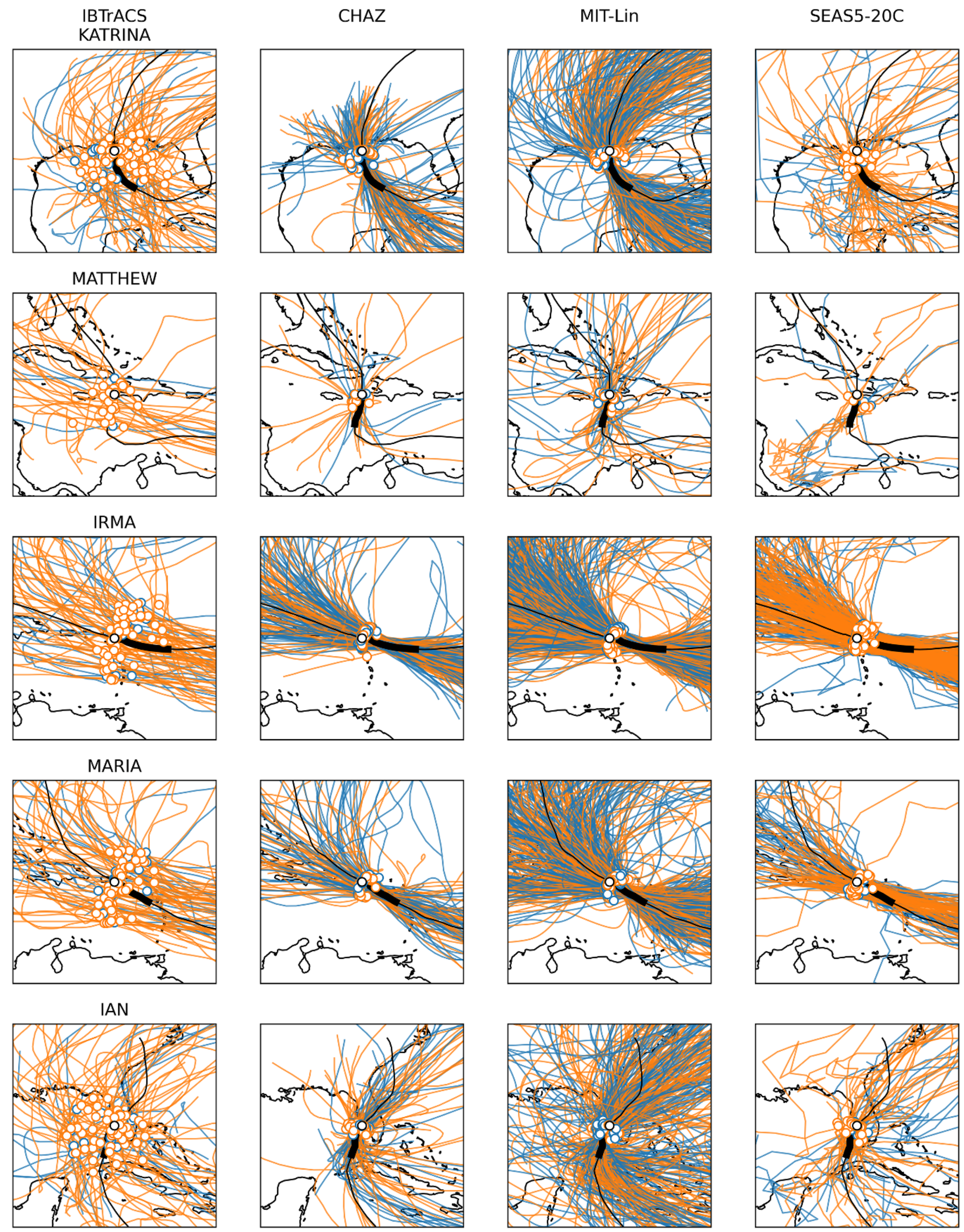

Figure A2. Same as figure 3 but for all 9 cases (continued in figure A3).

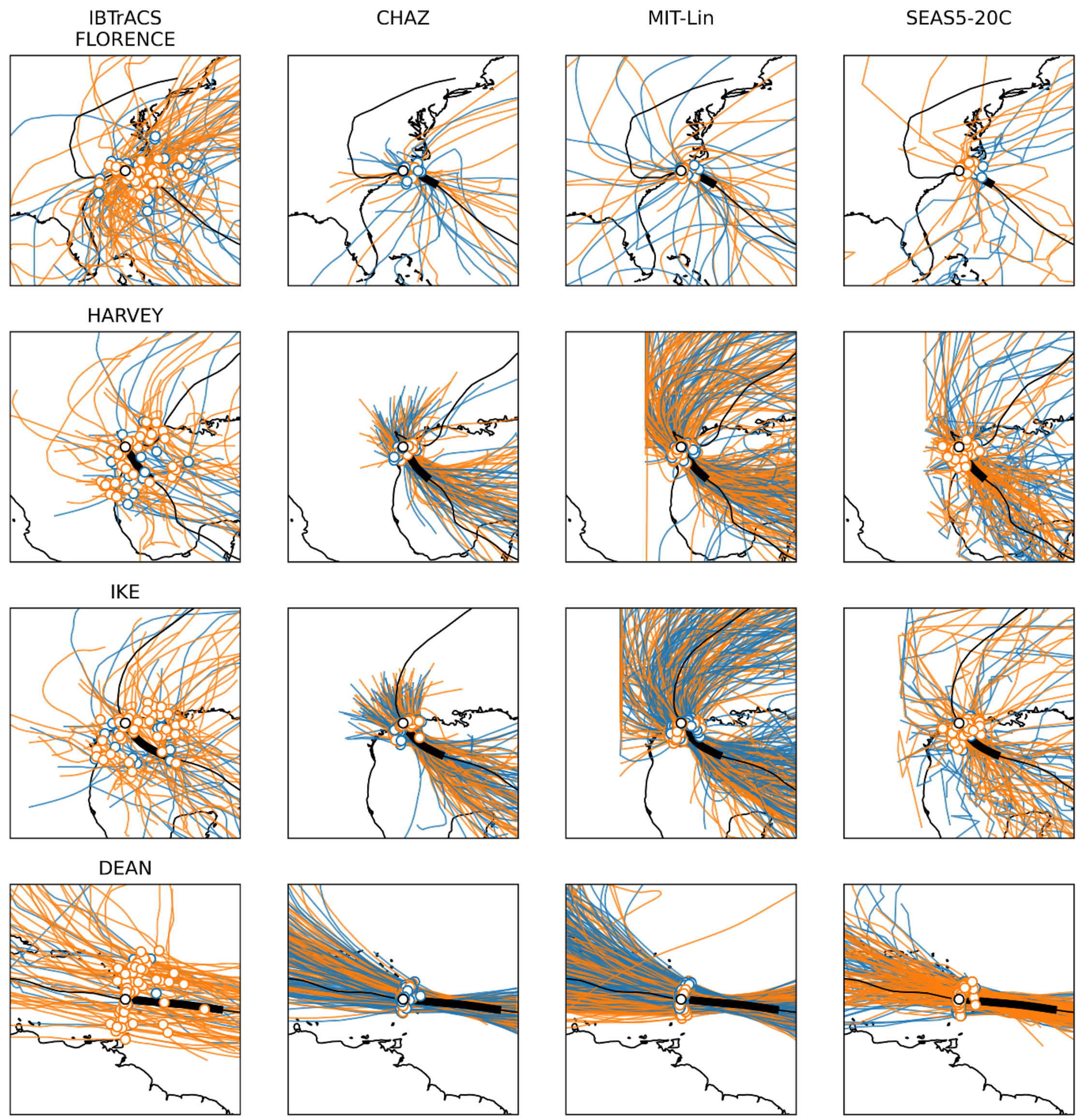

Figure A3. Same as figure 3 but for all 9 cases (continued from figure A2).

Table A6. p-values of the Cramer-von-Mises for difference in distribution of day-of-year in each period. Values below 5% are bolded with a star.

	IBTrACS	CHAZ	MIT	SEAS5
KATRINA	5.5×10^{-1}	1.1×10^{-1}	3.7×10^{-1}	6.4×10^{-1}
MATTHEW	5.1×10^{-2}	4.8×10^{-1}	5.4×10^{-1}	9.8×10^{-1}
IRMA	8.6×10^{-1}	$\mathbf{4.5\times10^{-2}}$*	5.3×10^{-1}	6.3×10^{-1}
MARIA	2.7×10^{-1}	4.8×10^{-1}	7.6×10^{-1}	3.4×10^{-1}
IAN	9.4×10^{-1}	1.8×10^{-1}	5.7×10^{-1}	4.0×10^{-1}
FLORENCE	$\mathbf{3.0\times10^{-2}}$*	5.0×10^{-1}	5.9×10^{-1}	6.6×10^{-1}
HARVEY	7.9×10^{-2}	6.9×10^{-1}	2.7×10^{-1}	1.6×10^{-1}
IKE	2.1×10^{-1}	2.8×10^{-1}	9.7×10^{-2}	9.9×10^{-1}
DEAN	2.5×10^{-1}	9.5×10^{-1}	7.9×10^{-1}	3.6×10^{-1}

ORCID iDs

Stella Bourdin https://orcid.org/0000-0003-2635-5654
Suzana J Camargo https://orcid.org/0000-0002-0802-5160
Chia-Ying Lee https://orcid.org/0000-0002-1644-375X
Mathieu Vrac https://orcid.org/0000-0002-6176-0439
Pradeebane Vaittinada Ayar https://orcid.org/0000-0001-8085-9621
Davide Faranda https://orcid.org/0000-0001-5001-5698

References

[1] IPCC 2021 Summary for policymakers *Climate Change 2021: The Physical Science Basis. Contribution of Working Group I to the Sixth Assessment Report of the Intergovernmental Panel on Climate Change* ed V Masson-Delmotte *et al* (Cambridge University Press) pp 1–31
[2] IPCC 2022 *Climate Change 2022: Mitigation of Climate Change. Contribution of Working Group III to the Sixth Assessment Report of the Intergovernmental Panel on Climate Change* (Cambridge University Press)
[3] Alexander L V *et al* 2024 *Front. Clim.* **6** 1455023
[4] Emanuel K 2003 *Ann. Rev. Earth Planet. Sci.* **31** 75–104
[5] Sobel A H, Wing A A, Camargo S J, Patricola C M, Vecchi G A, Lee C-Y and Tippett M K 2021 *Earth's Future* **9** e2021EF002275
[6] Knutson T *et al* 2020 *Bull. Am. Meteorol. Soc.* **101** E303–22
[7] Knutson T *et al* 2019 *Bull. Am. Meteorol. Soc.* **100** 1987–2007
[8] Vecchi G A, Landsea C, Zhang W, Villarini G and Knutson T 2021 *Nat. Commun.* **12** 4054
[9] Camargo S J *et al* 2023 *Trop. Cyclone Res. Rev.* **12** 216–39
[10] Kossin J P 2018 *Nature* **558** 104–7
[11] Lanzante J R 2019 *Nature* **570** E6–E15
[12] Wang C, Wu L, Lu J, Liu Q, Zhao H, Tian W and Cao J 2020 *J. Clim.* **33** 8641–50
[13] Yamaguchi M, Chan J C, Moon I-J, Yoshida K and Mizuta R 2020 *Nat. Commun.* **11** 47
[14] Hassanzadeh P, Lee C-Y, Nabizadeh E, Camargo S J, Ma D and Yeung L Y 2020 *Nat. Commun.* **11** 3319
[15] Kossin J P 2008 *Geophys. Res. Lett.* **35** 23
[16] Truchelut R E, Klotzbach P J, Staehling E M, Wood K M, Halperin D J, Schreck I I I C J and Blake E S 2022 *Nat. Commun.* **13** 4646
[17] Van Oldenborgh G J, Van Der Wiel K, Sebastian A, Singh R, Arrighi J, Otto F, Haustein K, Li S, Vecchi G and Cullen H 2017 *Environ. Res. Lett.* **12** 124009
[18] Risser M D and Wehner M F 2017 *Geophys. Res. Lett.* **44** 12–457
[19] Strauss B H, Orton P M, Bittermann K, Buchanan M K, Gilford D M, Kopp R E, Kulp S, Massey C, Moel H d and Vinogradov S 2021 *Nat. Commun.* **12** 2720
[20] Emanuel K 2017 *Proc. Natl Acad. Sci.* **114** 12681–4
[21] Wang S S, Zhao L, Yoon J-H, Klotzbach P and Gillies R R 2018 *Environ. Res. Lett.* **13** 054014
[22] Patricola C M and Wehner M F 2018 *Nature* **563** 339–46
[23] Reed K A, Stansfield A, Wehner M and Zarzycki C 2020 *Sci. Adv.* **6** eaaw9253
[24] Wang S Y S, Zhao L and Gillies R R 2016 *Geophys. Res. Lett.* **43** 11–805
[25] Jézéquel A, Yiou P and Radanovics S 2018 *Clim. Dyn.* **50** 1145–59
[26] Faranda D, Bourdin S, Ginesta M, Krouma M, Messori G, Noyelle R, Pons F and Yiou P 2022 *Weather Clim. Dyn. Discuss.* **2022** 1–37
[27] Faranda D *et al* 2024 *Weather Clim. Dyn.* **5** 959–83
[28] Hersbach H *et al* 2020 *Q. J. R. Meteorol. Soc.* **146** 1999–2049
[29] Dulac W, Cattiaux J, Chauvin F, Bourdin S and Fromang S 2024 *Clim. Dyn.* **62** 223–38
[30] Bourdin S, Fromang S, Dulac W, Cattiaux J and Chauvin F 2022 *Geosci. Model Dev.* **15** 6759–86
[31] Landsea C W and Franklin J L 2013 *Mon. Weather Rev.* **141** 3576–92
[32] Knapp K R, Kruk M C, Levinson D H, Diamond H J and Neumann C J 2010 *Bull. Am. Meteorol. Soc.* **91** 363–76
[33] Gahtan J, Knapp K, Schreck C, Diamond H, Kossin J and Kruk M 2024 NOAA National Centers for Environmental Information 10
[34] Lee C-Y, Tippett M K, Sobel A H and Camargo S J 2018 *J. Adv. Modeling Earth Syst.* **10** 223–41
[35] Tippett M K, Camargo S J and Sobel A H 2011 *J. Clim.* **24** 2335–57
[36] Camargo S J, Tippett M K, Sobel A H, Vecchi G A and Zhao M 2014 *J. Clim.* **27** 9171–96
[37] Emanuel K, Sundararajan R and Williams J 2008 *Bull. Am. Meteorol. Soc.* **89** 347–68
[38] Lee C-Y, Tippett M K, Camargo S J and Sobel A H 2015 *Mon. Weather Rev.* **143** 933–54
[39] Lee C-Y, Tippett M K, Sobel A H and Camargo S J 2016 *J. Clim.* **29** 7815–30
[40] Meiler S, Vogt T, Bloemendaal N, Ciullo A, Lee C-Y, Camargo S J, Emanuel K and Bresch D N 2022 *Nat. Commun.* **13** 6156
[41] Lin J, Rousseau-Rizzi R, Lee C-Y and Sobel A 2023 *J. Adv. Modeling Earth Syst.* **15** e2023MS003686
[42] Emanuel K 2006 *J. Clim.* **19** 4797–802
[43] Marks D G 1992 The beta and advection model for hurricane track forecasting *NWS Tech. Memo.* NWS NMC 70 National Meteorological Center (available at: https://repository.library.noaa.gov/view/noaa/7184)
[44] Emanuel K 2017 *Nat. Hazards* **88** 779–96
[45] Weisheimer A, Befort D J, MacLeod D, Palmer T, O'Reilly C and Strømmen K 2020 *Bull. Am. Meteorol. Soc.* **101** E1413–26
[46] Johnson S J *et al* 2019 *Geosci. Model Dev.* **12** 1087–117
[47] Weisheimer A, Balmaseda M and Stockdale T 2020 Multi-decadal variability in long-range enso predictions (seas5-20c) *EGU General Assembly Conf. Abstracts* p 7763
[48] Laloyaux P *et al* 2018 *J. Adv. Modeling Earth Syst.* **10** 1172–95
[49] Hodges K, Cobb A and Vidale P L 2017 *J. Clim.* **30** 5243–64
[50] Ginesta M, Flaounas E, Yiou P and Faranda D 2024 *J. Clim.* **37** 5427–52
[51] Yang Q, Lee C-Y, Tippett M K, Chavas D R and Knutson T R 2022 *Weather Forecast.* **37** 477–93
[52] Done J M, Ge M, Holland G J, Dima-West I, Phibbs S, Saville G R and Wang Y 2020 *Nat. Hazards Earth Syst. Sci.* **20** 567–80
[53] Schreck C J, Knapp K R and Kossin J P 2014 *Mon. Weather Rev.* **142** 3881–99
[54] Faranda D, Ginesta M, Alberti T, Coppola E and Anzidei M 2023 *npj Clim. Atmos. Sci.* **6** 181